Chapter 11
Fatigue Crack Growth under Variable-Amplitude Loading

Symbols

CA	Constant Amplitude
VA	Variable Amplitude
OL	Overload
UL	Underload
a	crack length
β	geometry correction factor
C, m	constants in Paris relation
K	stress intensity factor

11.1 Introduction

Fatigue under Variable-Amplitude (VA) loading was discussed in the previous chapter. Key words of the discussion were: prediction of fatigue life until failures, the Miner rule and its shortcomings, fatigue damage of cycles with an amplitude below the fatigue limit, residual stress effects due to notch root plasticity, and service-simulation fatigue tests as an alternative to Miner

rule predictions. The fatigue life was supposed to include the crack initiation period and the crack growth period until failure. It was tacitly assumed that the crack growth period was relatively short and could be disregarded. The present chapter is dealing with the growth of macrocracks under VA loading. The crack initiation period dealing with crack nucleation and microcrack growth is not addressed.

The propagation of macrocracks is a significant issue if fatigue cracks cannot be avoided, especially if safety or economy is involved. Dangerous situations can occur in pressure vessels, high-speed rotating masses (turbine disks, blades of wind turbines) and aircraft structures as some characteristic examples. Incidental cracks can be generated by a variety of conditions; such as surface damage, corrosion pits, material defects in welded joints, inferior production quality, etc. Furthermore, the fatigue life of a structure in service may cover many years. The occurrence of macrocracks can then be acceptable in order to avoid a low design stress level and a corresponding heavy structure.

Microcracks usually have a negligible effect on the ultimate strength of a structure, but macrocracks will substantially reduce the static strength. Obvious questions are: (i) How fast are these cracks growing? (ii) Is it possible to find the cracks by periodic inspections? Because of these arguments the prediction of fatigue crack growth under CA and VA loading has received much attention in the literature. Crack growth under CA loading was discussed in Chapter 8. Crack growth under VA loading is the subject of the present chapter. Significant interaction effects can occur during the growth of macro cracks, and as a consequence, sequence effects are also possible. However, there are essential differences with fatigue at notches. Notch root plasticity and fatigue damage increments of cycles below the fatigue limit were considered in the previous chapter. In the present chapter crack tip plasticity, crack closure and the significance of cycles with a low ΔK-value are discussed for VA-load histories.

Crack growth under simple VA-stress histories is discussed in Section 11.2 to illustrate and explain the occurrence of crack growth retardation and acceleration. Effects of the load history, material yield stress and material thickness are discussed. Plasticity induced crack closure is significant for explaining the interaction effects. Crack growth under complex VA-stress histories is discussed in Section 11.3. Crack growth prediction models for VA loading are considered in Section 11.4, followed by an evaluation in Section 11.5. The major topics of the present chapter are summarized in Section 11.6.

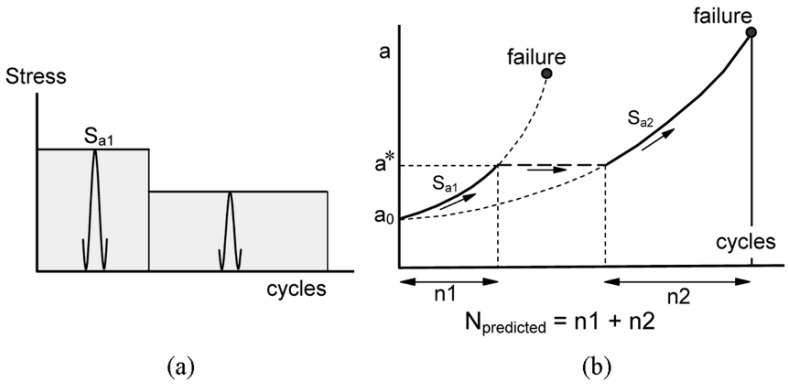

Fig. 11.1 Non-interaction fatigue crack growth in a two-block VA test.

11.2 Crack growth under simple VA-stress histories

Most investigations on fatigue crack growth under VA-stress histories were carried out on aircraft materials: strong Al-alloys, Ti-alloys and high-strength low-alloy steels. Significant work has also been done on low-carbon steels because fatigue crack growth is of interest to large welded structures. Many VA crack growth tests were carried out with simple load histories in order to see whether fatigue crack growth was delayed or accelerated by a change of the stress amplitude. The effect of single high load cycles was also abundantly studied. These high loads have a very large effect on crack growth. Although the simple load histories in these test series are different from service load histories, the experiments have significantly contributed to the present understanding of interaction and sequence effects during fatigue crack growth. The understanding is essential for developing crack growth prediction models for VA loading discussed in Section 11.4.

Non-interaction behavior

Fatigue crack growth under VA loading would be simple if crack growth in every cycle was dependent on the severity of the current cycle only, and not on the load history in the preceding cycles. A most simple case to be considered here is crack growth under a load history with two blocks of CA cycles as shown in Figure 11.1a. Fatigue crack growth under the high-stress amplitude S_{a1} starts from an initial crack length a_0 until a crack length a^* is obtained. The stress amplitude is then reduced to S_{a2} and the test is continued

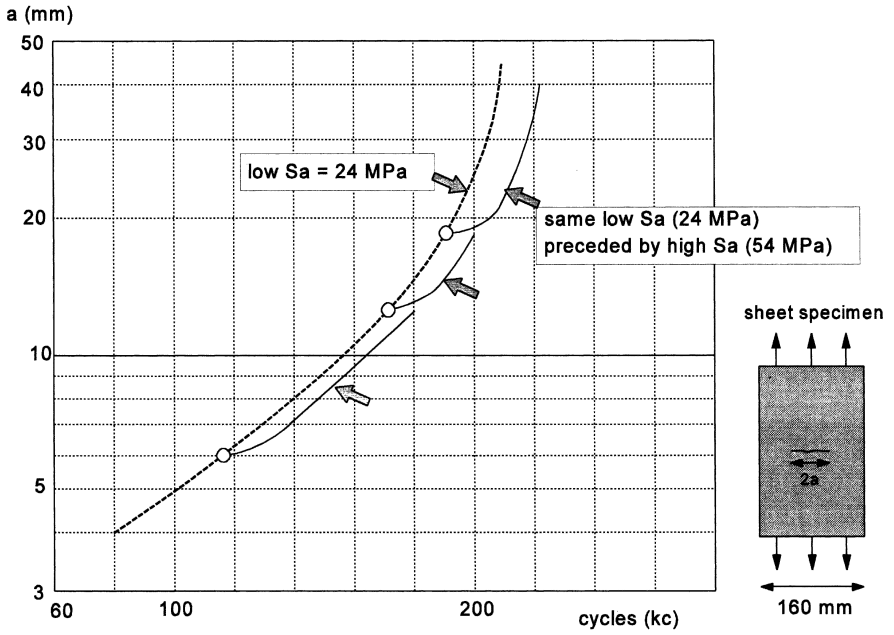

Fig. 11.2 Grack growth test on 2024-T3 Al-alloy specimens ($S_m = 80$ MPa). Crack growth retardation after transitions from a high amplitude to a lower amplitude [1].

until failure. The CA crack growth curves for both amplitudes are shown in Figure 11.1b. If crack growth at the second amplitude would not depend on how the crack has grown until a^*, the initial growth along curve 1 is continued along curve 2, and the total crack growth life is $n_1 + n_2$. This prediction implies that n_1 and n_2 are predicted in the same way as it should be done for CA loading as discussed in Chapter 8. Unfortunately, experimental evidence has shown that crack growth in the second block is affected by crack growth in the first block. An illustration of this interaction effect is shown in Figure 11.2. After the transition of a high amplitude (54 MPa) to a low amplitude (24 MPa), crack growth was retarded during a crack growth increment of 1 to 3 mm. The crack growth curves then were again parallel to the original crack growth curve of the low amplitude. The crack growth rate was no longer reduced and the retardation was over.

Effects of OL cycles

Much larger retardations are observed in tests with a high peak load added to CA loading. Such high loads are frequently called overloads

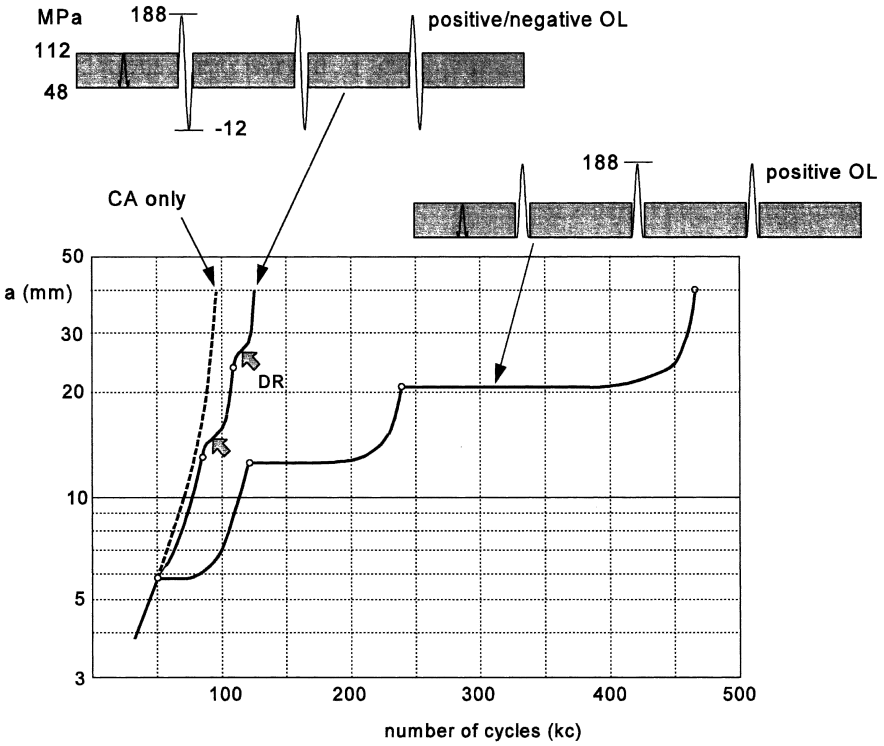

Fig. 11.3 The effect of overloads (OL) on fatigue crack growth in sheet specimens of the aluminium alloy 2024-T3 [1] ($S_m = 80$ MPa). (DR = delayed retardation)

(OL). Figure 11.3 shows the crack growth curve for a test with three high OLs. After the application of each peak load, a most significant delay of fatigue crack growth occurred. The original crack growth life with the CA loading only was just below 100 kc. However, with the three peak loads the crack growth life was almost 500 kc. These crack growth retardations are generally attributed to plasticity induced crack closure (the Elber mechanism) discussed in Chapter 8 (Section 8.4.1). The crack closure phenomenon is a consequence of plastically elongated material left in the wake of the crack by previously created crack tip plastic zones, see Figure 8.10. This phenomenon implicates crack closure at a positive gross stress. A load cycle with a high maximum stress causes a relatively large plastic zone and thus will leave more plastic deformation in the wake of the crack after further crack growth. It increases the crack tip opening stress level, S_{op}, and thus reduces the effective stress intensity range (ΔK_{eff}). The lower ΔK_{eff} explains the crack growth retardation in Figure 11.2. However,

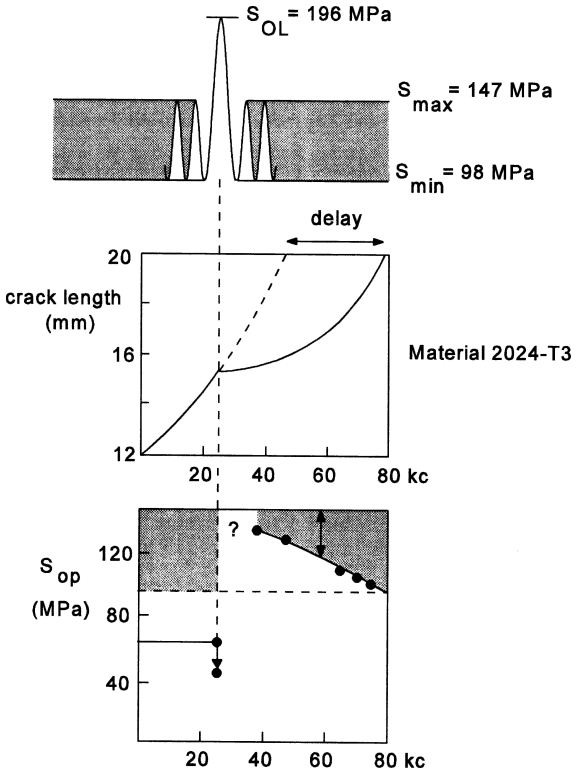

Fig. 11.4 Crack growth retardation after an OL and the relation with S_{op} [2].

the peak loads in Figure 11.3 have caused a relatively large plastic zone, and as a result much more crack closure when the crack tip was penetrating into these zones. This concept was confirmed by some elementary tests carried out by Arkema [2]. Crack closure measurements were made during a CA test ($R = 0.67$) with a single OL as shown in Figure 11.4. The delay caused by the OL can easily be observed from the crack growth curve. Crack closure measurements carried out before the application of the OL indicated $S_{op} \sim 62$ MPa. Immediately after the OL, the S_{op}-level was reduced to about 45 MPa because the OL is opening the crack by crack tip plasticity. Crack closure measurements after some further crack growth indicate a significantly increased S_{op}-values above S_{min} of the CA cycles. As a result, reduced ΔS_{eff}-values occur, and crack growth retardation is observed. After S_{op} decreased to $S_{op} = S_{min}$, the crack growth delay was over because crack closure no longer occurs during the following CA cycles. Although the crack

closure measurements may have a limited accuracy, the trend of Figure 11.4 is considered to be correct.

Figure 11.3 also shows a crack growth curve of a specimen subjected to three OLs, but with the OL immediately followed by a large negative amplitude load, also called underloads (UL). There is still some crack growth retardation, but the large effect of the OLs was drastically reduced. Again the results can be explained by considering plasticity induced crack closure. The OL creates a relatively large crack tip plastic zone which also leads to crack tip blunting. Because of the open crack tip after the OL, reversed plastic deformation occurs at the crack tip during the application of the UL until the crack tip is closed again. In this reversed plastic zone, residual tensile stresses are present and crack growth retardation should not be expected. On the contrary, some crack growth acceleration is possible in this small reversed plastic zone. However, as discussed in Section 8.4.1, the reversed plastic zone is smaller than the monotonic plastic zone of the preceding OL, see Figure 8.10. After the crack tip has passed the reversed plastic zone and enters the monotonic plastic zone of the OL cycle, some crack growth retardation is possible again. This phenomenon is called delayed retardation because it required some crack extension before it becomes effective. Delayed crack growth retardation is addressed again later.

Difference between cracks and notches

An essential difference between cracks and notches should be noted here. During crack growth, compressive loads can reduce the favorable effect of tensile peak loads, but it does not necessarily lead to a reduced crack growth life. Macro cracks can already be closed during a decreasing load when the load is still a tension load. A closed crack is no longer a stress raiser, and significant negative plastic strains in the crack tip plastic zone do not occur. However, if a notch is loaded under compression, the notch is not closed. It remains a stress raiser, and notch root plasticity can introduce unfavorable residual tensile stresses with an adverse effect on fatigue life as discussed in the previous chapter (Section 10.2.2).

Effect of material thickness

Crack growth retardation after an OL should depend on the size of the plastic zone because crack closure is induced by crack tip plasticity of the OL.

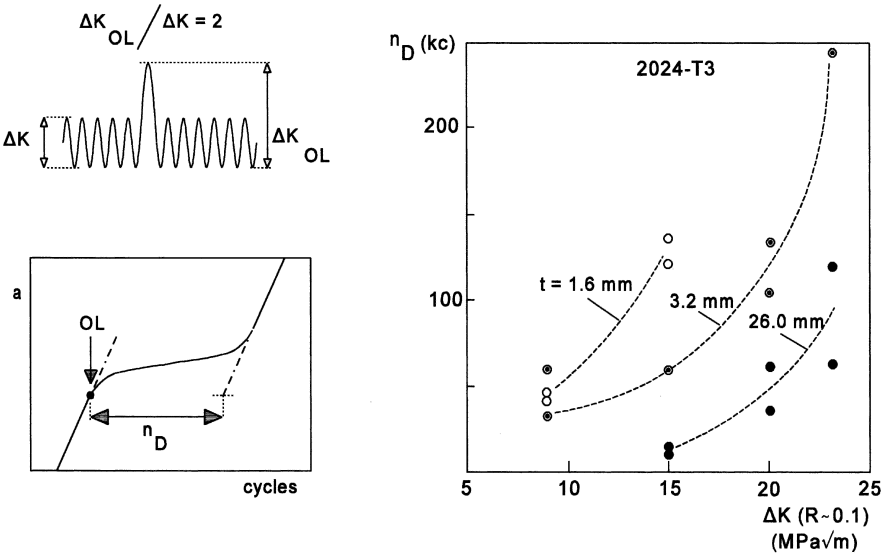

Fig. 11.5 Effect of material thickness on the crack growth delay period after a single OL. Constant-ΔK tests on 2024-T3 specimens. Results of Mills and Hertzberg [3].

Recall, the size of the plastic zone is different for plane strain and for plane stress, see Section 5.8. In a thin sheet, the state of stress at the crack tip is predominantly plane stress; whereas, in a thick plate it is predominantly plane strain. Plastic zones are larger in thin sheets. It then should be expected that the retardation effects are different for fatigue cracks in thin sheets and thick plates. This was confirmed by results of Mills and Hertzberg [3], see Figure 11.5. They carried out crack growth tests with a constant ΔK instead of a constant ΔS. It requires that $S_{\max}$ and $S_{\min}$ are continuously reduced during crack growth to maintain a constant R-value. This can be done automatically during a fatigue test, see Chapter 13. As a result of the constant ΔK, a constant crack growth rate $\mathrm{d}a/\mathrm{d}N$ is observed. An OL cycle inserted in a constant-ΔK test systematically reduces the crack growth during a period of crack growth retardation. After some crack growth, the growth rate returned to its original constant value. The delay period (n_D cycles) can then be defined in a simple way, see the inset figure in Figure 11.5. Two trends are obvious from the test results: (i) The delay period is larger for thinner material (larger plastic zone) for a given ΔK, see, for instance, the results in Figure 11.5 at $\Delta K = 15$ MPa$\sqrt{\mathrm{m}}$. (ii) The delay period increases at higher stress intensities of the OL (larger plastic zones). These trends agree with

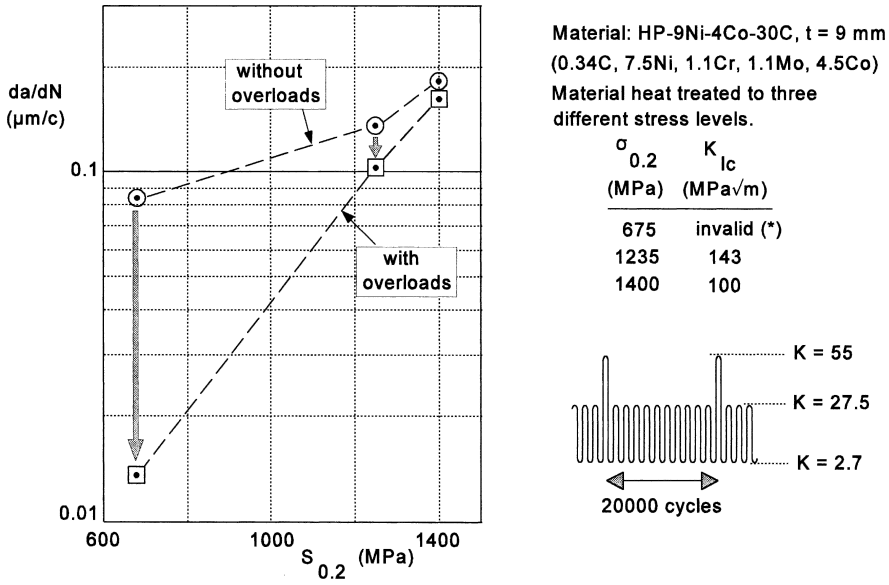

*A valid K_{Ic} cannot be measured if the plastic zone is too large compared to the specimen thickness, see ASTM Standard E399.

Fig. 11.6 Effect of material yield stress on crack growth retardation by periodic OL cycles. Results of Petrak [4].

the effect of the plastic zone size on crack closure and thus on crack growth retardation.

Effect of material yield stress

An instructive example is shown in Figure 11.6 by the results of Petrak [4] for a high-strength steel. The material was heat treated to three different yield stress levels. Petrak also carried out constant-ΔK tests, but he introduced periodic OL cycles after each 20000 cycles. In tests without peak loads, the crack growth rate was larger if the steel was heat treated to a higher yield stress. Apparently, the alloy was more sensitive for fatigue crack growth at a higher strength of the material (recall the discussion in Chapter 8). The periodic OL cycles reduced the crack growth rate. The reduction was large for a low yield stress material (larger plastic zone) and much smaller for the high yield stress material (small plastic zone). Also, this observation confirms the significance of the plastic zone size of OLs for subsequent crack growth retardation.

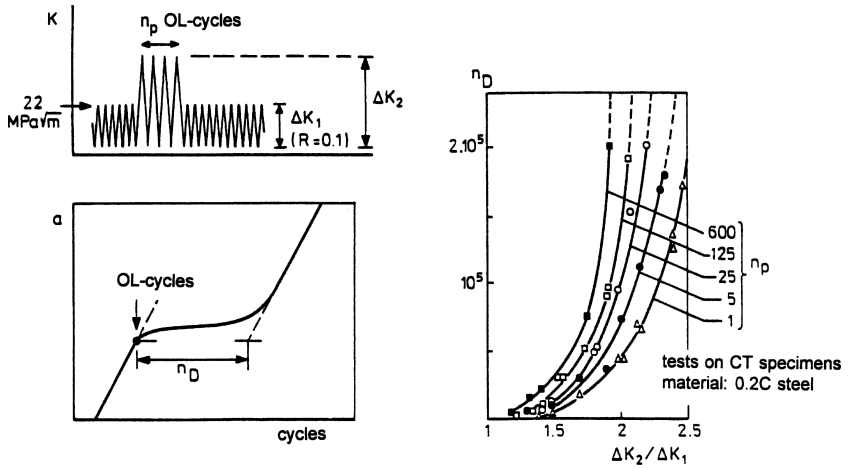

Fig. 11.7 The effect of the number of OL cycles (n_p) on the crack growth delay period (n_D). Results of Dahl and Roth [5].

Block of OL cycles

As discussed above, one OL cycle can give a considerable delay of crack growth. However, it has also been observed that more OL cycles give a larger delay. Illustrative results for a low-carbon steel are presented in Figure 11.7. Dahl and Roth [5] also carried out constant-ΔK tests and adopted the same delay period definition as Mills and Hertzberg (Figure 11.5). The test results show that the delay period is larger for higher OLs. However, it is noteworthy that larger numbers of OL cycles systematically increased the delay period. Crack extension occurs during the OL cycles. More OL cycles thus will leave more plastic deformation in the wake of the crack behind the crack tip. This explanation is based again on the Elber crack closure mechanism. The phenomenon of a larger delay by more OL cycles is called a multiple OL effect.

Delayed retardation

Retardation after an OL may require some crack growth before a maximum reduction of the crack growth rate is obtained, see Figure 11.8. Delayed retardation was observed in several investigations, but the observation is not easily made because this delay occurs during a small crack length increment only. As discussed before in relation to Figure 11.3, an OL can lead to a blunted and open crack tip. This will reduce S_{op} and facilitates the

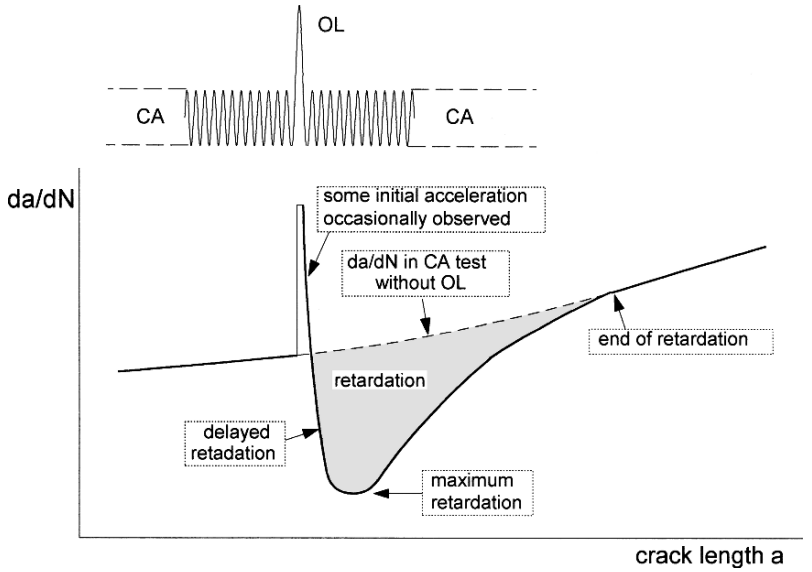

Fig. 11.8 Delayed retardation after an overload (OL).

very beginning of growing into the new crack tip plastic zone of the OL. Moreover, some crack growth acceleration can then occur due to residual tensile stress in the reversed plastic zone (Figure 8.10). The residual tensile stress promotes crack tip opening. The acceleration directly after the OL is observed during a small crack length increment. Further crack growth into the OL plastic zone meets with increasing crack closure as a result of residual compressive stresses introduced by the OL in the monotonic plastic zone (Figure 8.10). A decreasing crack growth rate is observed. Because the minimum crack rate does not occur immediately after the OL, the term "delayed retardation" was introduced. After passing the minimum crack growth rate and some substantial further crack extension, the growth rate returns to the normal CA crack growth rate of the CA base line cycles. The size of the OL plastic zone is important for the crack extension during which retardation is observed. But the end of retardation does not necessarily occur at the edge of this plastic zone as sometimes suggested for crack growth prediction models. Moreover, it should be recalled that the boundary of the plastic zone is not an accurately defined concept. The plastic zone estimates of Equations (5.35) and (5.36) are actually primitive estimates, based on one single dimension and disregarding the shape of the plastic zone. Furthermore, the plastic zone size estimates adopt $S_{0.2}$ as a criterion for the boundary between elastic and plastic material around the crack tip. However,

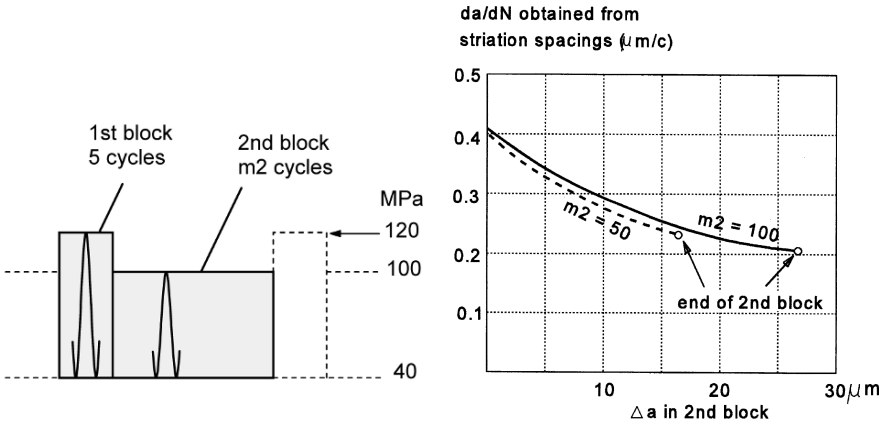

Fig. 11.9 Delayed retardation in second block of low-amplitude cycles. Sheet specimen of the Al-alloy 2024-T3.

a yield stress $S_{0.1}$ (0.1% plastic deformation) as sometimes used in the UK, would lead to larger calculated plastic zone sizes.

The more reliable indications on delayed retardation should come from striation observations. In this respect Al-alloys are instructive because they show striations better than most other alloys. Illustrative results have been obtained in tests with periodic blocks of larger and smaller cycles, see Figure 11.9 [6]. Five larger cycles were followed by 50 or 100 smaller cycles. The striation spacings indicated a decreasing crack growth rate. Delayed retardation apparently occurred, but a minimum crack growth rate was not yet reached before the next block of high-amplitude cycles was applied.

Crack growth retardation by crack closure or residual stress in the crack tip plastic zone?

Dahl and Roth [5] raised the question whether crack growth delay after an OL is due to crack closure, or whether there is also an effect of the residual compressive stress in the plastic zone ahead of the crack tip. An interesting CA experiment was carried out by Błazewicz [7]. He made ball impressions on 2024-T3 sheet specimens before the crack growth test was started, see Figure 11.10. As a result of the plastic deformation, residual compressive stresses were present in a zone between the ball impressions. This caused crack growth retardation. The delay was small during the growth through the zone between the impressions, but it was significant at a later stage.

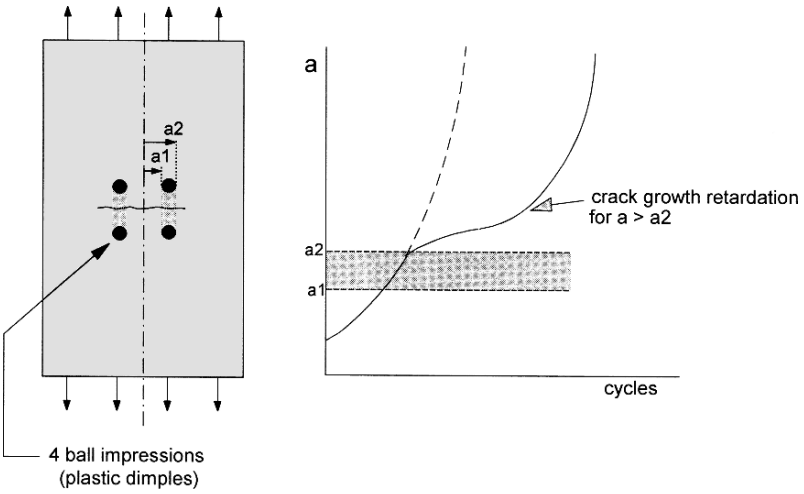

Fig. 11.10 Crack growth retardation in CA test by residual stress created in the wake of the crack by ball impressions. Measurements of Błazewicz [7].

It suggests that crack growth retardation should primarily be explained by the crack closure and opening phenomenon. In terms of the crack growth mechanism, it is logical that the crack must be opened before crack extension can start. The retardation for $a > a_2$ in Figure 11.10 thus indicates that crack tip opening was less than normal. This is a consequence of the excess of material in the wake of the crack. The retardation cannot be related to residual stresses ahead of the crack tip.

More crack closure at the material surface

At the surface of a material, the crack tip is loaded under plane stress conditions. Depending on the material thickness, the state of stress at mid thickness is approaching plane strain conditions. The plastic zone size under plane stress is significantly larger than under plane strain. As discussed in Chapter 5 (Section 5.8) the Irwin plastic zone size estimates are $r_p = (1/\alpha\pi) \cdot (K/S_{0.2})^2$, with $\alpha = 1$ for plane stress and $\alpha = 3$ for plane strain. It thus should be expected that crack closure is more significant near the material surface, and will occur to a lesser degree at mid thickness. This is confirmed by FEM calculations [8], but there is also experimental confirmation [9, 10]. McEvily [11] studied crack growth after an OL in Al-alloy specimens (6061), which gave a significant crack growth delay. In another test, he reduced the thickness of the specimen from 12.7 to 6.3 mm

immediately after the OL by removing plate surface material on both sides of the specimen. A much smaller crack growth retardation was then found as compared to the crack growth delay without removing surface material. As already discussed in Chapter 8 (Section 8.4.2), it confirms that crack closure occurs predominantly at the material surface, and much less at mid thickness of a material. This implies a significant complication for prediction models for crack growth under VA loading.

Incompatible crack front orientation under VA loading

Interaction effects during fatigue crack growth under simple VA-load histories as discussed before, were qualitatively explained by considering the occurrence of crack closure. It was recognized that plane strain/plane stress problems were present, which implies that crack closure is predominantly occurring at the material surface. Plane stress is associated with a free surface. The same is true for the occurrence of shear lips discussed in Chapter 2 (Section 2.6 and Figure 2.38). If shear lips are developed under CA loading, which occurs for several technical materials, it can lead to a transition from a tensile-mode crack to a shear-mode crack. The development of shear lips depends on the crack driving force, ΔK. It implies that shear lips occur earlier at high stress amplitudes. The maximum width of the shear lips is half the material thickness. As a consequence, the full transition from the tensile mode to the shear mode is more evident in thin sheet material.

Under VA loading, the development of shear lips and the transition to the shear mode can imply incompatible crack front orientations, a topic rarely covered in the literature. A simple example is shown on the fracture surface in Figure 11.11. The fatigue cracks at both sides of a central notch (width 3 mm) were growing during cycles with $S_a = 50$ MPa. An increasing shear lip width can be observed. The crack were already fully in the shear mode when a block of low-amplitude cycles ($S_a = 25$ MPa) was introduced. It caused a narrow bright band on the fracture surface (arrows in Figure 11.11). The normal fracture mode of the low-amplitude cycles under CA loading at that particular crack length is the tensile mode (with minute shear lips). This is not compatible with the existing shear mode introduced by the high-amplitude cycles. A tendency to return to the tensile mode could be observed which gave the bands a faceted appearance. The growth rate in the bands was eight times lower than recorded in normal CA-tests at the same crack length, which is a significant retardation.

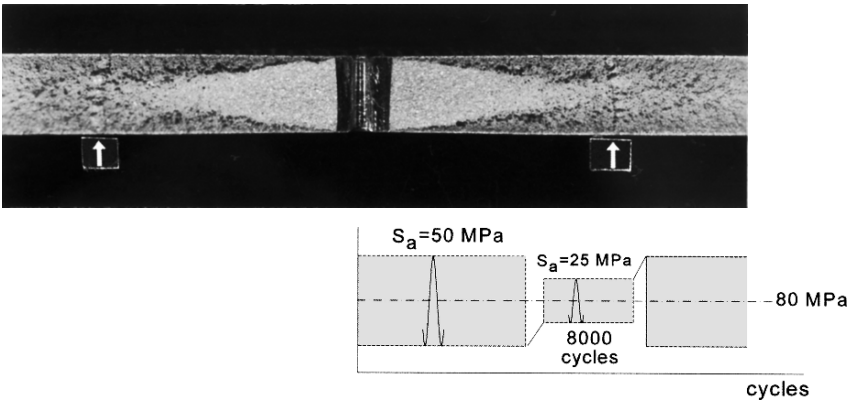

Fig. 11.11 Fatigue fracture surface of an Al-alloy (2024-T3) specimen with a central crack, thickness 4 mm. Crack growth in the first block of cycles produced shear lips until the entire crack front was in the shear mode. Crack growth in the second block with low-amplitude cycles then occurred with an incompatible crack front orientation [12].

The reverse case is perhaps more relevant, i.e. when high-amplitude cycles occur between many low-amplitude cycles. The fracture surface then can be largely in the tensile mode, whereas the failure mode corresponding to the nominal ΔK cycle of the high-amplitude cycle in a CA test may be the shear mode, or at least a mixed mode with significant shear lips. In elementary tests [12], such large cycles produced dark bands on the fracture surface, and a growth rate far in excess of the corresponding CA results. In this case the incompatible crack front orientation caused an increased crack growth rate during the high-amplitude cycles.

Another incompatibility can occur if different crack growth mechanisms apply to low and high stress amplitudes. Some materials, for instance Ti-alloys, can exhibit structurally sensitive crack growth at low amplitudes, and a more regularly flat crack growth at a high amplitude. If low amplitudes and high amplitudes occur, a mismatch (incompatibility) can occur, and thus lead to interaction effects. An interesting proof was given in fracture toughness tests of Stubbington and Gun [13]. Fatigue crack growth at a low $K_{\max}$-value (10.8 MPa$\sqrt{\text{m}}$) produced a rough fatigue fracture surface (structurally sensitive crack growth), whereas crack growth at a high $K_{\max}$ (19.1 MPa$\sqrt{\text{m}}$) gave a flat fracture surface (structurally insensitive crack growth). In the former case, the rough crack in a static test gave a fracture toughness $K_{Ic} = 72.9$ MPa$\sqrt{\text{m}}$, whereas in the latter case, the flat crack gave a significantly lower $K_{Ic} = 49.3$ MPa$\sqrt{\text{m}}$. A similar phenomenon can occur in other materials during fatigue crack growth after an OL. The

initial crack growth after the OL occurs extremely slowly in a plastic zone with severe plastic deformations and possibly void formation. Fractographic observations in the electron microscope have shown a rather distorted crack growth path after the OL. On a micro scale, the crack front is rather irregular and crack growth is more difficult, not only due to plasticity induced crack closure, but also because the crack driving energy must propagate a more complex and longer crack front.

11.3 Crack growth under complex VA-stress histories

The discussion in the previous section on crack growth under simple VA-stress histories has shown that plasticity induced crack closure (Elber mechanism) is the major mechanism responsible for interaction effects during the growth of macro cracks. Complications are associated with plane stress/plane strain aspects and with possible incompatibilities between crack growth mechanisms for low and high stress amplitudes. Although the interaction effects usually lead to crack growth retardation, crack growth acceleration is sometimes possible. All these observations can also occur under complex VA-stress histories. The following topics are discussed in this section:

- Sequence effects.
- Thickness effects.
- Initial fast crack growth at a notch.
- Truncation effects.

Sequence effects

Ryan [14] studied fatigue crack growth in a high-strength D6AC steel under Lo-Hi-Lo program loading at $R = 0$, see Figure 11.12. As a result of the stepwise amplitude changes, fatigue bands could be observed on the fracture surface for each block of the symmetric program. The crack growth rates could then be calculated from the measured width of the bands. It turned out that the crack growth rate was smaller in the Hi-Lo part of a period than in the Lo-Hi part, see the results in Figure 11.12. This figure also contains the $\mathrm{d}a/\mathrm{d}N$ curve for CA loading which confirms that crack growth retardation occurred in the Hi-Lo part of the period, and crack growth acceleration in the Lo-Hi part, including the maximum amplitude of the program. In view

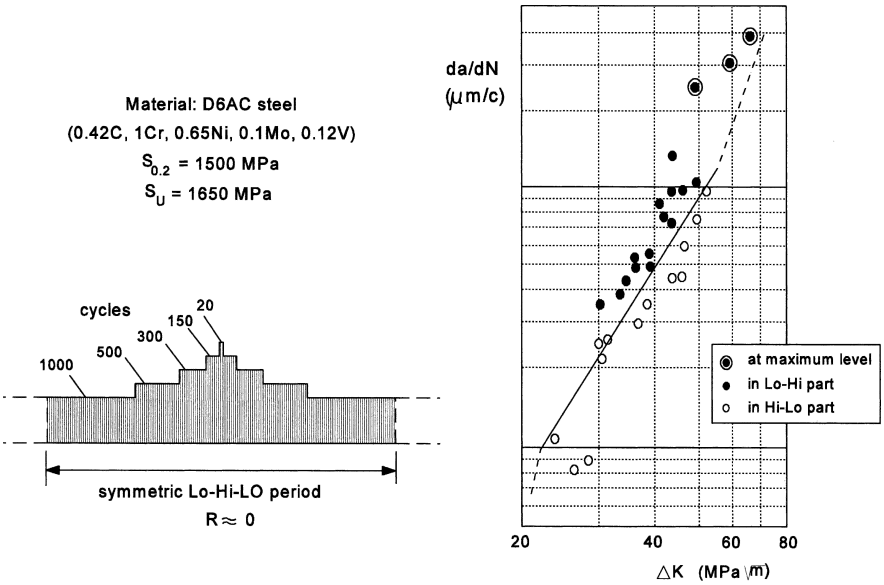

Fig. 11.12 Sequence effects during crack growth in a high-strength steel under program fatigue loading. Results of Ryan [14].

of the $R = 0$ condition, the block of the 20 largest cycles should be expected to have a favorable effect on crack growth in the following cycles with a lower $S_{\max}$. In terms of crack closure, S_{op} during the decreasing S_a cycles will be higher than in CA tests. During the increasing part of the sequence, S_{op} will be lower and the crack growth rate will be higher.

Another illustrative test program was carried out on fatigue crack growth in 2024-T3 sheet material [15]. The load spectrum used was based on a spectrum for air turbulence on a wing of a transport aircraft wing. The spectrum contains 40000 cycles with seven different amplitudes. The spectrum with the same load cycles was used with two random sequences and some programmed sequences, see Figure 11.13. The random sequences were applied with full cycles, i.e. each cycle consisted of two half cycles with the same amplitude. However, in one random load history, each cycle started with the positive half cycle followed by the negative one. In the other random load history this sequence was reversed. As shown by the results in the upper part of Figure 11.13, the difference between the crack growth lives of the two random load test series was small.

In the program fatigue tests with the full spectrum in one period (40000 cycles), the results in the lower part of Figure 11.13 indicate two remarkable trends. (i) There is a systematic sequence effect with the longer crack growth

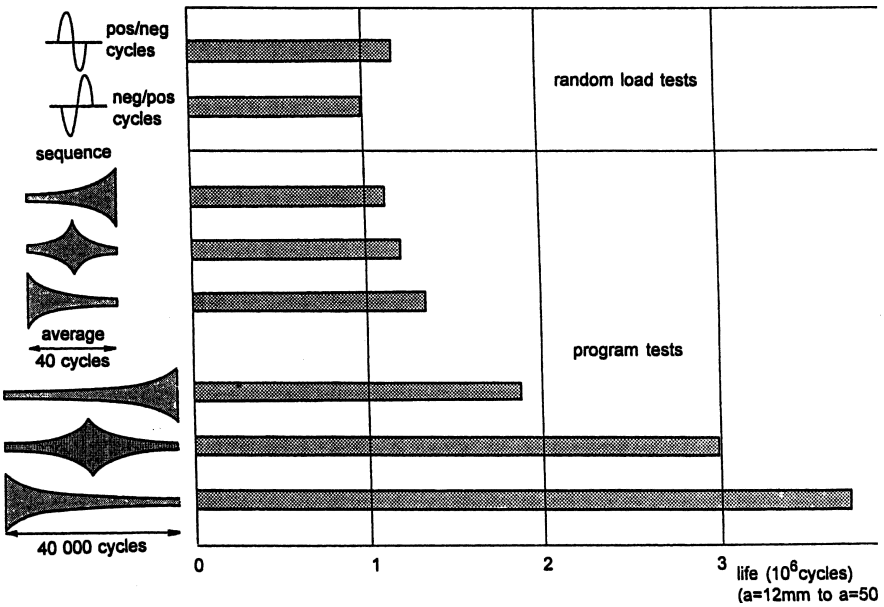

Fig. 11.13 A comparison between fatigue crack growth lives under random loading and different types of program loading [15]. Sheet material 2024-T3, $S_m = 69$ MPa.

life for the Hi-Lo sequence, a shorter life for the Lo-Hi sequence, and an intermediate life for the Lo-Hi-Lo sequence. The explanation given for the fractographic results of Ryan (Figure 11.12) also applies to these results. (ii) Even more remarkable, and actually disturbing, the crack growth lives were considerably longer than for the random sequence, i.e. about three times longer for the Lo-Hi-Lo sequence. It implies that the program fatigue tests give an unconservative result for a random sequence! Fractographic observations indicated that the fracture surfaces of these program fatigue tested specimens were more irregular than the fracture surfaces obtained under the random sequences. It then should be concluded that fatigue crack growth is just not the same phenomenon for these programmed and random sequences of the same cycles.

In the third group of tests, programmed sequences were used again, but now with a much shorter period (average of 40 cycles). In order to accommodate the full 40000 cycles spectrum in these tests, not all periods could be similar. Some periods contained also the rarely occurring high-amplitude cycles, while other periods did not. The sequence of the periods of different severity was random again. The crack growth life results were of the same order of magnitude as for the fully random

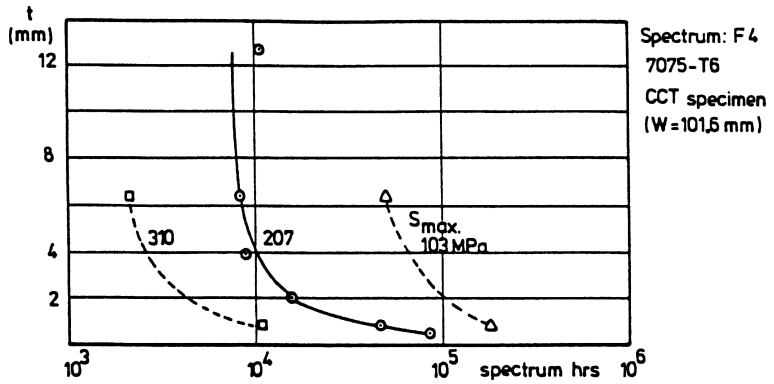

Fig. 11.14 Material thickness effect on crack growth life under flight-simulation loading. Results of Saff and Holloway [16].

sequence. The fracture surface appearance was also similar. The important lesson is that a load spectrum with a random load sequence in service should not be simulated by a programmed sequence with a long period. A programmed sequence with a long period is an artificial simulation, which as a simplification cannot be accepted. A similar conclusion was already drawn in the previous chapter on fatigue life problems including the crack initiation period.

Thickness effect

Saff and Holloway [16] carried out flight-simulation fatigue tests with a load spectrum based on a maneuver loads (F-4 aircraft). Crack growth was observed in center cracked tension specimens of different thicknesses varying from 0.5 to 12.7 mm. For a maneuvre spectrum the maximum stress occurring in the flight-simulation test is used as the characteristic stress level. Three stress levels were used. The results in Figure 11.14 clearly show a systematic thickness effect, i.e. lower endurances for thicker material. As discussed in the previous section, an increased thickness leads to more plane strain at the crack front, and thus to smaller plastic zones, less crack closure and less crack growth retardation. As a consequence, the crack growth lives are smaller. The life for the thin sheet material was about 10 times(!) longer than for the thick plate material. A similar thickness effect was also found in flight-simulation tests with a gust spectrum [17].

A thickness effect on fatigue crack growth is sometimes observed in CA tests, but in general the effect is larger for VA-load histories. It must be

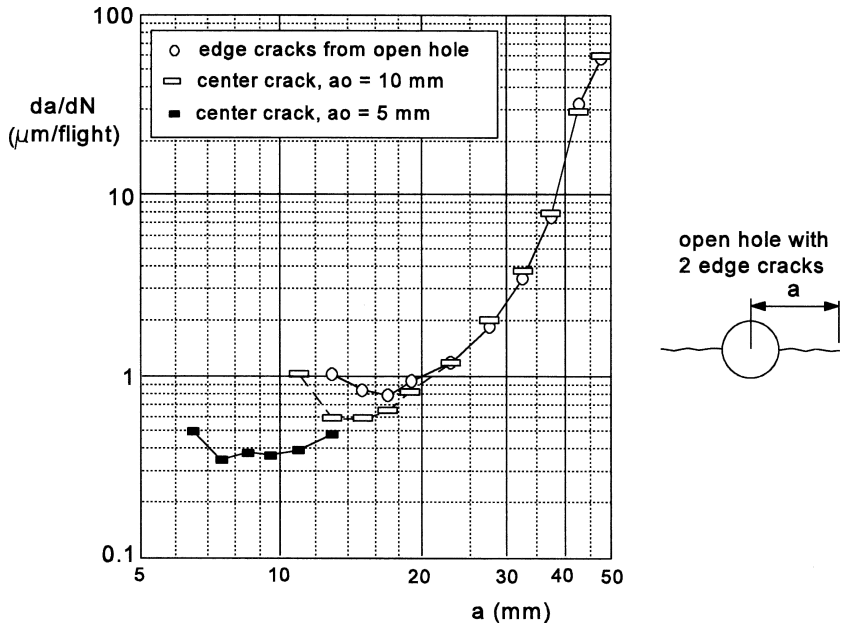

Fig. 11.15 Initial fast crack growth at the edge of a hole. Flight-simulation loading with gust load spectrum (F-28) [18]. Sheet material 2024-T3, $S_{mf} = 69$ MPa.

concluded that representative crack growth experiments should not only be based on a realistic load history, but a relevant material thickness should also be used.

Initial fast crack growth at a notch

Figure 11.15 shows the crack growth rate of a crack starting at the edge of an open hole (radius 5 mm) in a specimen loaded by a flight-simulation load history. It is quite remarkable that the crack growth rate initially decreased to a minimum at $a = 17$ mm. Decreasing of the crack rate occurred in spite of a nominally increasing stress intensity associated with an increasing crack length. After some further crack growth the expected increase of the crack growth rate occurred. Crack growth under the same flight-simulation loading was also recorded for cracks which were not initiated at the edge of a hole. They started as an extension of a fatigue crack obtained under CA loading at a low load level to have a low crack opening stress level (S_{op}). Crack growth during subsequent flight-simulation loading started again with a decreasing crack growth rate, see the results of two tests in Figure 11.15. After passing

a minimum growth rate, the increasing parts of all tests nicely line up along the same growth rate curve. It should be concluded that the initial decrease of the growth rate should be associated with the development of a plastic wake field behind the crack tip. A substantial plastic wake field did not yet exist in the first period of the crack growth life. It requires some crack growth during which the maximum peak loads of the load spectrum can build up significant plasticity in the wake of the crack.

The behavior of an initially decreasing crack growth rate has been observed in various flight-simulation fatigue tests (e.g. [19]), but an initially decreasing growth rate of hole edge cracks under CA loading was also observed by Broek [20]. However, for VA loading the phenomenon can be more important, especially for steep load spectra with low numbers of high-amplitude cycles (see Figure 9.10), and less important for materials with a relatively high yield stress because of smaller crack tip plastic zones. Anyway, an important lesson to be learned from the above experience is that artificial fatigue crack starters may not give realistic information of the early crack growth rates.

Load spectrum truncation effect

In the previous chapter (Section 10.4.5) it was discussed that truncation of rarely occurring high load amplitudes can have a large effect on the fatigue life, especially for steep load spectra with rarely occurring high loads. This is also true for the propagation of macro cracks, probably still more than for notch fatigue problems. A steep load spectrum is applicable to wing structures of transport aircraft. Figure 11.16 shows results of crack growth tests on Al-alloy 2024-T3 sheet specimens (width 100 mm, thickness 2 mm) loaded at a mean stress in flight $S_{mf} = 70$ MPa. The gust spectrum is a rather steep spectrum, which implies that high loads are relatively rare, see Figure 11.16a. The highest gust level is reached once in 4000 flights. The lower levels II, III, IV and V are reached 3, 8, 26 and 78 times per 4000 flights respectively, while the total number of cycles in 4000 flights is about 400000. As shown by the crack growth curves in Figure 11.16b, truncation of the high amplitudes to lower levels significantly reduced the crack growth life. The crack growth life for truncation level V is about 7 times shorter than the life for truncation level II. Tests at truncation level I, the highest one in Figure 11.16a, were stopped because the growth rate was very low.

Similar truncation effects on fatigue crack growth have been found for different Al-alloys, a Ti-6Al-4V alloy and a high-strength steel (survey

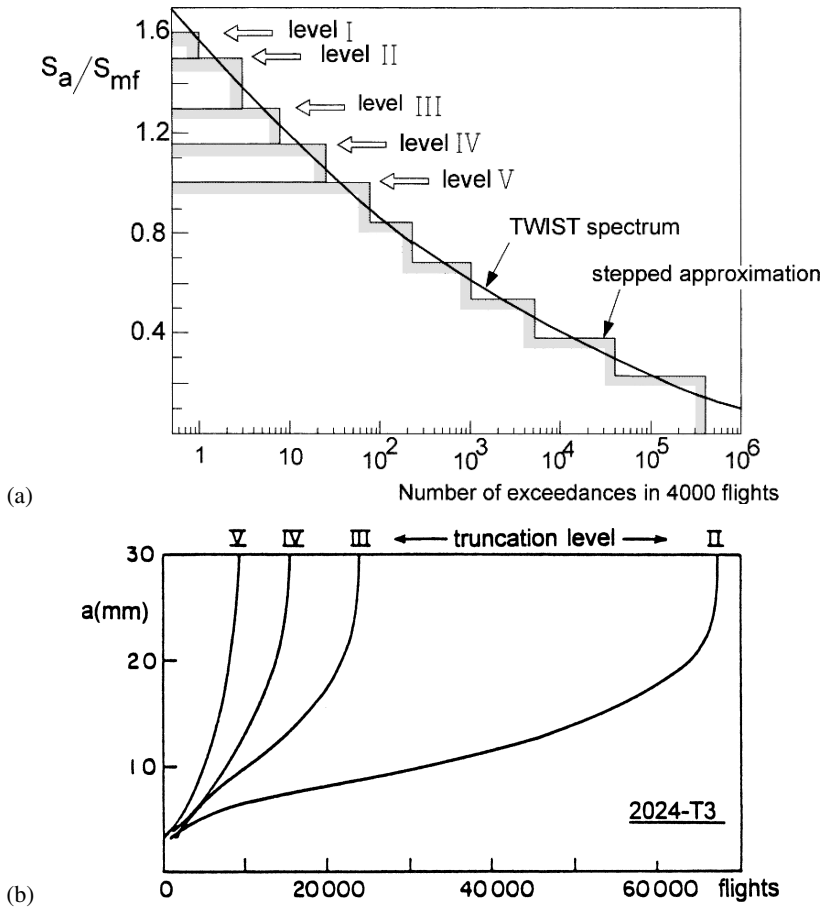

Fig. 11.16 Effect of spectrum truncation on crack growth in 2024-T3 Al-alloy sheet specimens under flight-simulation loading [21].

in [22]). However, it appears that the truncation effect is smaller for the 7075-T6 alloy, which could be associated with the higher yield stress of the material ($S_{0.2} \approx 475$ MPa for 7075-T6 and $S_{0.2} \approx 350$ MPa for 2024-T3). Plastic crack tip zones are smaller and as a result the retardation effects can be less significant. The important point is that truncation effects can occur. These effects were also noted for less steep spectra. The choice of a suitable truncation level must be given due attention if service simulation fatigue tests are carried out. A high truncation level, i.e. including load cycles with a very high amplitude, will give longer fatigue lives and lower crack growth rates. These results can be unconservative because not all structures in service will meet these high-amplitude loads.

11.4 Crack growth prediction models for VA loading

The literature on prediction models for fatigue crack growth under VA loading is extensive. Observations on crack growth retardation after OLs, and the occurrence of crack closure have stimulated the development of several prediction models. In general, these models predict fatigue crack propagation as a cycle-by-cycle process. In view of striation observations, this seems to be logical. Crack growth is assumed to be a summation of Δa-values, or

$$a_n = a_0 + \sum_{i=1}^{i=n} \Delta a_i \tag{11.1}$$

The value of a_n is the crack length after n cycles, a_0 is the initial crack length, and Δa_i is the crack extension Δa in cycle number i. Some comments related to Equation (11.1) should be made:

(i) The crack extension in a cycle is an equilibrium between a "crack driving force" and a "crack growth resistance", see the discussion in Section 8.6.1. The crack driving force in prediction models is expressed in terms of the stress intensity factor. This factor can only be defined if there is a crack of some length. It implies that the prediction with Equation (11.1) should always start with a finite crack length; a_0 cannot be zero. As a consequence, the crack nucleation life cannot be predicted by fracture mechanics methods based on K-values.

(ii) Further to the previous remark, an additional comment must be made on the minimum value of a_0 which can be used in crack growth predictions. As discussed in Chapter 2, the transition from the crack initiation period to the crack growth period is dependent on the type of material and the structure of the material. As long as the growth of a microcrack is still a structurally sensitive phenomenon at the material surface, predictions based on K-values are not justified. This problem was discussed earlier in Section 8.6.1 on fatigue crack growth under CA loading.

(iii) The crack extension in a cycle is per definition the crack growth rate in that cycle. As a consequence, the prediction should be a cycle-by-cycle prediction of the crack growth rate. This occurs in the prediction models still to be discussed. But, models differ in the way of predicting the crack growth rate in every cycle.

(iv) Equation (11.1) assumes that the size of the crack is fully defined by a single size parameter, the crack length a. As discussed in Chapter 8 for a part-through crack with a curved crack front, the shape of the crack must be accounted for by a variation of K along the crack front.

11.4.1 Non-interaction model

The most simple prediction model is the non-interaction model. Crack growth in each cycle is assumed to be independent of the preceding load history which has created the crack. This option was already discussed in Section 11.2 and illustrated with Figure 11.1. It was pointed out that this approach is physically unrealistic because considerable interactions have been reported. Crack growth retardations and accelerations can occur during VA loading. Retardations are the more likely phenomena. Thus, if interaction effects are ignored, it may be expected that non-interaction predictions are conservative. Prediction can even be highly conservative for a steep load spectrum with occasional high loads, and probably less conservative for a flat spectrum with many high amplitude cycles.

The non-interaction approach leads to a simple numerical summation with Equation (11.1) and values $\Delta a = \mathrm{d}a/\mathrm{d}N$ as obtained in CA tests. Such crack growth data should be available as a function of ΔK, including the stress ratio effect:

$$\Delta a_i = f(\Delta K_i, R) \tag{11.2}$$

The equation was previously discussed as Equation (8.3) in Chapter 8. The crack growth data can be available as an analytical function (see Section 8.3), but CA crack growth data in tabular format can also be used with interpolation between these data. Computer algorithms can be written to obtain crack growth results with Equations (11.1) and (11.2). This should not be difficult if interaction effects in the VA-stress history are supposed to be absent.

One restriction should be made on using CA crack growth data. Contributions of cycles with a very low ΔK are supposed to be zero if the ΔK-value is below the nominal threshold value ΔK_{th} of macro-cracks, see Figure 8.6. The growth of cracks in the threshold region was discussed in Section 8.3, and it was pointed out that the determination of a ΔK_{th}-value has a problematic character. This value is obtained in experiments with a decreasing crack growth rate until the crack driving force can no longer overcome the crack growth resistance. Under these threshold conditions it can lead to an erratic crack growth mechanism, which may not be representative for crack growth under VA loading. It may be expected that cycles with $\Delta K < \Delta K_{\mathrm{th}}$ can still contribute to crack growth because these cycles were not preceded by some erratic crack growth mechanism occurring in threshold experiments. It is recommended to extrapolate the $\mathrm{d}a/\mathrm{d}N$-ΔK data in the Paris region to lower ΔK-values in the threshold region as shown

in Figure 8.6. Although the extrapolation has no solid physical background it still appears to be more reasonable and safer than ignoring this aspect. The problem has a certain similarity to the problem of extrapolating S-N curves below the fatigue limit for fatigue life predictions with the Miner rule for VA-load histories.

11.4.2 Interaction models for prediction of fatigue crack growth under VA loading

Different prediction models for fatigue crack growth under VA loading are associated with different concepts about crack tip plastic zones and crack closure. Three groups of models are listed in Table 11.1. The early yield zone models, do not consider crack closure. They account for interaction effects by assumptions about plastic zone sizes. Later the crack closure models include predictions on the occurrence of crack closure, but still with assumptions about crack closure stress levels during VA loading. The strip yield models are the most advanced models. Crack closure stress levels are obtained by calculations rather than assumptions.

Originally, the prediction models were mainly verified for through cracks in sheet and plate specimens of aluminium alloys, but later experiments were also done on other materials. The models are considered to be applicable for high-strength alloys with a limited ductility. Actually, these materials are the most fatigue critical materials. Mild steel is not in this category. Due to its special yielding behavior and its high ductility, mild steel is a class of materials of its own. Fatigue crack growth in low-C steel under VA loading is becoming an increasingly relevant problem because of welded structures. Essential features of the three types of models listed in Table 11.1 will be briefly summarized.

Table 11.1 Three categories of crack growth prediction models.

Type of model	Crack closure used?	Crack closure relation
Yield zone models	no	–
Crack closure models	yes	empirical
Strip yield models	yes	calculated

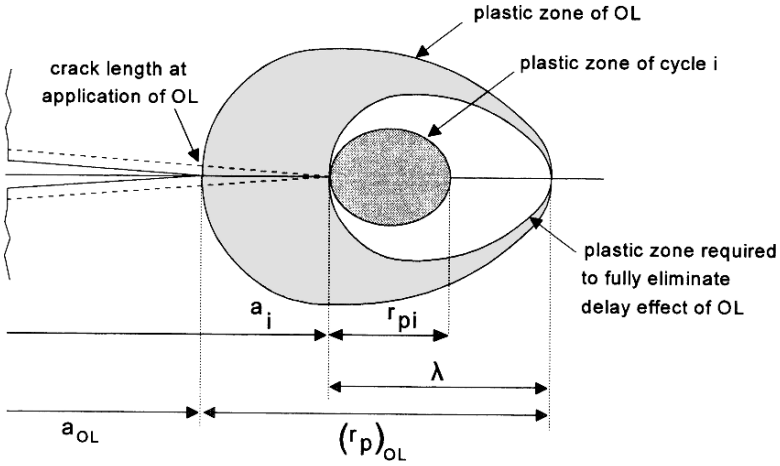

Fig. 11.17 Plastic zone size definition used in the models of Willenborg [23] and Wheeler [24].

Yield zone models

The models of Willenborg [23] and Wheeler [24] were proposed to explain crack growth delays caused by high loads. The models consider the plastic zone sizes indicated in Figure 11.17, but the concepts are different. In both models, it was recognized that new plastic zones are created inside the large plastic zone of an OL. Moreover, the possibility was considered that these new plastic zones could be large enough to extend beyond the OL plastic zone. The Willenborg model starts from a strange assumption, which implies that crack growth delay after an OL is due to a reduction of $K_{\max}$ instead of a reduction of ΔK_{eff}. This seems to be physically incorrect. Crack closure in the model is supposed to occur only if $K_{\min} < 0$. From a mechanistic point of view, the Willenborg model does not agree with the present understanding of crack closure.

Wheeler introduced a retardation factor γ defined by

$$\left(\frac{\mathrm{d}a}{\mathrm{d}N}\right)_{\text{VA}} = \gamma \cdot \left(\frac{\mathrm{d}a}{\mathrm{d}N}\right)_{\text{CA, same K-cycle}} \tag{11.3}$$

The amplification factor γ is assumed to be a power function of the ratio r_{pi}/λ_i, with $r_{p,i}$ as the current plastic zone size created by the cycle considered, and γ as the distance between the crack tip and the edge of the OL plastic zone, see Figure 11.17.

$$\gamma = \left(\frac{r_{p,i}}{\lambda}\right)^m \tag{11.4}$$

If $r_{p,i}$ is large enough to be equal to λ, then $\gamma = 1$ and according to Equation (11.3) the delay effect of the OL is gone. The exponent m is an empirical constant dependent on the type of the VA-load history. It must be determined by VA-load experiments for each load history of interest.

The Willenborg model and the Wheeler model can predict crack growth retardation only ($\gamma < 1$), not acceleration. After an OL, the maximum retardation occurs immediately. Delayed retardation is not predicted. Modifications of the two models have been proposed in the literature, which has led to more empirical constants. Plasticity induced crack closure is not considered. It appears that both models have fundamental limitations in predicting the crack growth behavior under VA loading discussed in Sections 11.2 and 11.3.

Crack closure models

The crack closure models account for the occurrence of plasticity induced crack closure (Elber mechanism). The values of S_{op} in each cycle of the stress history is predicted. The current value depends on the preceding fatigue crack growth and corresponding plastic wake field of the fatigue crack. A cycle-by-cycle variation of S_{op} as shown in Figure 11.18 must be predicted. The effective stress range in a cycle is $\Delta S_{\text{eff}} = S_{\max} - S_{\text{op}}$. The corresponding ΔK_{eff}-range in cycle i becomes

$$\Delta K_{\text{eff},i} = \beta_i \Delta S_{\text{eff},i} \sqrt{\pi a_i} \tag{11.5}$$

with β_i as the geometry correction factor, depending on the momentary crack length a_i. The predicted crack extension in the cycle is:

$$\Delta a_i = \left(\frac{\mathrm{d}a}{\mathrm{d}N}\right)_i = f(\Delta K_{\text{eff},i}) \tag{11.6}$$

If the Paris relation should be valid, the equation becomes

$$\Delta a_i = C(\Delta K_{\text{eff},i})^m \tag{11.7}$$

Crack growth then follows from the summation of Δa_i according to Equation (11.1).

The main question about the crack closure models is how the variation of S_{op} is predicted for a VA-laod history. Four crack closure models proposed in the literature are briefly commented upon:

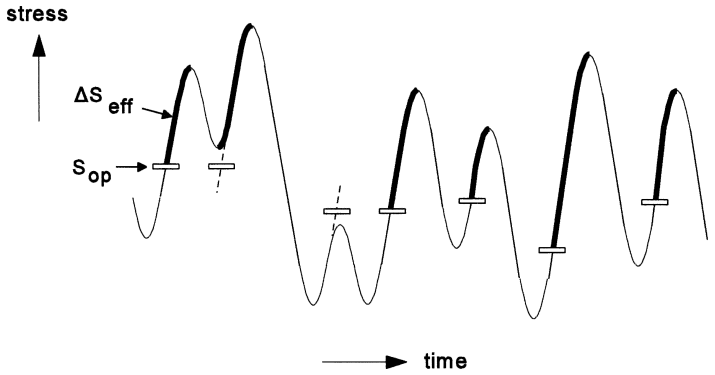

Fig. 11.18 VA loading with cycle-by-cycle variations of S_{op}.

- the ONERA model [25],
- the CORPUS model [26],
- the modified CORPUS model [27], and
- the PREFFAS model [28].

The models were developed primarily for aircraft fatigue problems with applications to flight-simulation load histories, such as illustrated in Figure 9.25. The variation of S_{op} during the flight-simulation load history depends on the preceding load history. It implies that information, characteristic for the previous load history, must be stored in a memory file. The characteristic information is associated with the larger positive and negative peak loads. These loads have introduced significant plastic zones and reversed plasticity which can increase or decrease S_{op} of later cycles. There are significant differences between the models, which will not be discussed here in detail. The reader is referred to the original publications and a survey presented by Padmadinata [27, 29]. However, some comments are made to illustrate essential features of these models.

The PREFFAS model is the simplest model. The CORPUS model of De Koning [26] is the most detailed one. De Koning also presents the most explicit picture about crack closure between the crack flanks. He assumes that it does occur at the larger plastic zones in the wake of the crack left by plastic deformation of the more severe loads. The somewhat protruding zones are called “humps”. A hump can be “flattened” by later downward loads which implies a reduction of S_{op}. Various differences between the models are associated with assumptions made for the plane strain/plane stress transition during crack growth, calculation of the plastic zone sizes, empirical equations for calculating S_{op} (Elber type relations), decay of S_{op}

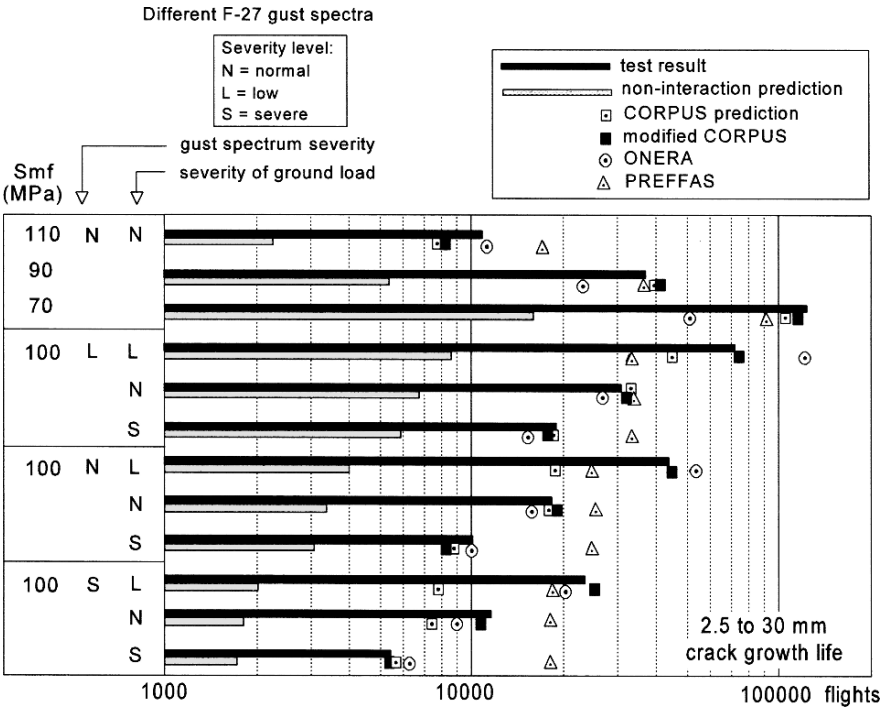

Fig. 11.19 Comparison between test results and prediction on fatigue crack growth life under flight-simulation loading (compiled with data of [27]). Sheet specimens of 2024-T3 Alclad, thickness 2 mm.

during crack growth, multiple overload effect, and method of deriving S_{op} from the previous load history. An analysis and comparison of the models was made by Padmadinata [27, 29] with extensive verifications primarily for realistic flight-simulation load histories and test results of the two Al-alloys, 2024-T3 and 7075-T6. Simplified flight-simulation tests were also included. As an example, predicted fatigue lives for crack growth from 2.5 to 30 mm under realistic flight- simulation loading are compared to test results in Figure 11.19. The test variables include the stress level, characterized by the mean stress in flight (S_{mf}), gust spectrum severity, and severity of the ground load during landing. The test results show that the effects of these variables agrees with expectations; i.e. more severe conditions lead to shorter crack growth lives.

Non-interaction predictions are also shown in Figure 11.19, which unfortunately is not always done in model verifications. A comparison between non-interaction predictions and the test results is made in order see whether significant interactions occurred. The results in Figure 11.19 clearly

indicate the occurrence of significant interaction effects. The test results are much larger than the non-interaction predictions; on average about five times larger crack growth lives. This could be expected because the load spectrum in the flight-simulation fatigue tests was a gust spectrum, a steep spectrum with rarely occurring high loads. Figure 11.19 also shows that the prediction of all crack closure models are reasonably close to the test results. Some more comments on the predicted results can be made:

- The PREFFAS model does not predict any effect of the severity of the ground load, because all negative loads are clipped to zero. However, the test results show a systematic effect of the ground stress level.
- The predictions of the CORPUS and ONERA models are fairly close to the test results. The test results indicate a significant reduction of the crack growth life for a more severe ground stress level. This trend in not always correctly predicted by the CORPUS model if the gust spectrum is severe. In the latter case, the maximum downward gust load, occurring only once in 2500 flights, is a larger compressive load then the ground load occurring in every flight. This rarely occurring gust load overrules the negative effect of the ground load. This was the reason to modify the CORPUS, which led to the modified CORPUS model [27]. The model is still largely the same as the original CORPUS model, but it introduces a modified memory for downward loads to give a better prediction for the test conditions in the flight-simulation tests [27, 29].

The CORPUS model was verified by Ichsan [30] for semi-elliptical surface cracks in plate specimens of Al-alloys. The analysis included a variation of S_{op} along the crack front. A satisfactory agreement was found between predictions and test results including the development of the crack front shape.

The agreement between predictions and test results, as illustrated by Figure 11.19 appears to be promising, but it must be admitted that the agreement is largely limited to crack growth under specific aircraft load spectra and typical aircraft materials. Furthermore, although the models are based on the physically relevant crack closure phenomenon, they still include several plausible assumptions and adjustment in order to come to a better correspondence between prediction and empirical proof. An analysis of the models indicates some typical issues not yet resolved, such as:

- Crack growth retardation after OLs is predicted, but delayed retardation is not predicted. According to the models, the maximum retardation starts immediately after the overload, which is in conflict with empirical evidence.

- Plane strain/plane stress transitions are included in the CORPUS and the ONERA model, although not in the same way. It leads to a thickness effect, but variations along the crack front are averaged. The transition is not included in the PREFFAS model, but the model requires empirical data for the OL effect representative for the thickness considered.
- Multiple OL effects are accounted for in the CORPUS and the ONERA model, although not in the same way. The CORPUS model predicts an increasing S_{op} during the beginning of stationary flight-simulation loading, which is necessary to predict the initially decreasing crack growth rate (Figure 11.15).
- Incompatible crack front orientations and related phenomena are not covered.

Strip yield models

The previous crack closure models are based on the occurrence of crack closure in the wake of the crack. Assumptions had to be made to account for crack closure under VA loading, but plastic deformation in the wake of the crack is not calculated. This was done in some FE studies [31, 32] which confirmed the occurrence of crack closure and simple interaction effects to be expected in qualitative agreement with empirical observations. Because such calculations cannot be made for many cycles, the Dugdale strip yield model [33] was adopted to calculate the plastic zone size and the plastic extension of the material in this zone. This type of work was started by Führing and Seeger [34, 35]. Quantitative strip yield models were proposed by Dill and Saff [36, 37], Newman [38], De Koning et al. [39], and Wang and Blom [40]. Later modifications were proposed by Bos [41] and Skorupa and Machniewicz [42].

In the Dugdale plastic zone model, plastic deformation occurs in a thin strip with a rigid perfectly plastic material behavior. Plastic extensions of strip elements in the plastic zone are calculated by considering the opening of a fictitious crack with a tip at the right edge of the plastic zone in Figure 11.20. The crack opening depends on the remotely applied load and the yield stress applied in the plastic zone on the fictitious crack tip flanks. Because the crack grows into the plastic zone, a plastic wake field is created, which can induce crack closure at positive stress levels. The models are rather complex, which is a consequence of the non-linear material behavior and the occurrence of closing and opening of the crack. Reversed plastic deformation in the wake field can occur when the crack is closed and locally

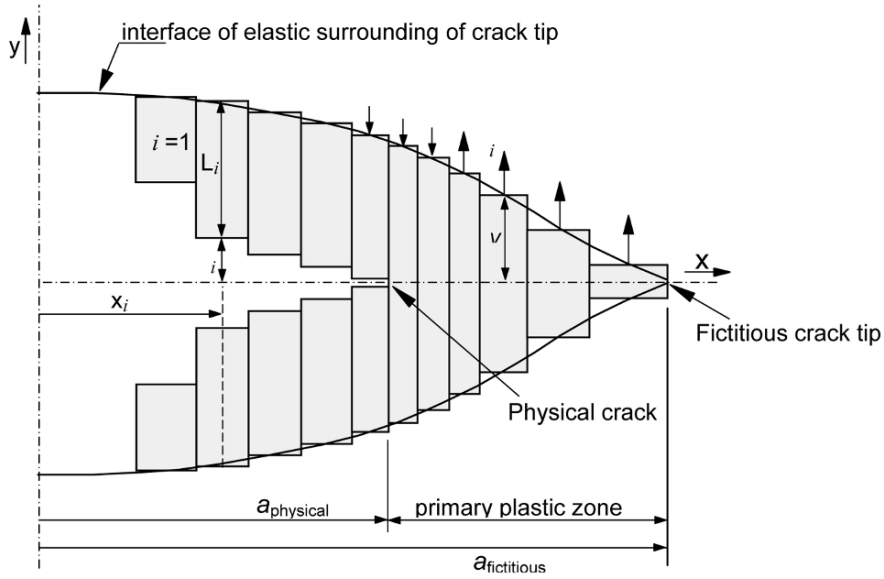

Fig. 11.20 Crack tip in a strip yield model [43].

under compression. Stresses and deformations for the strip elements are solved iteratively by considering compatiblity conditions along the fictitious crack surface. Plane strain/plane stress transitions are included by changing the yield stress used in the Dugdale model. It has led to a so-called plastic constraint factor α, which is used to tune the predictions to be in agreement with experimental data. Several predictions are reported for both simple tests with overload/underload cycles and flight-simulation tests. In general the agreement is considered to be good.

Strip yield models are not discussed here in detail, but some remarks are made, partly in comparison to the crack closure models:

- Empirical equations on crack closure levels are replaced by calculation of S_{op} as a function of the history of previous plastic deformations. Elber's assumption that $U(R)$ is independent of the crack length is no longer necessary.
- Delayed retardation is predicted [43].
- In the strip yield model of De Koning, his concept of primary and secondary plastic zones is introduced [44], which accounts for large Δa-values of peak load cycles, see the discussion in Section 11.5.
- Multiple OL effects should occur in a strip yield model if the modeling is sufficiently refined.

- The plane strain/plane stress transition is still covered by assumptions.
- Incompatible crack front interactions are not covered.

Strip yield models are superior to the crack closure models because the physical concept has been improved. The calculation of the crack driving force, i.e. ΔK_{eff}, is based on calculations of the history of the plastic deformations in the crack tip zone and in the wake of the crack. Several problems of these models still require further analysis. The models have not yet widely been verified.

11.5 Evaluation of prediction methods for fatigue crack growth under VA-load histories

Engineering aspects

Some predominant characteristics of fatigue crack growth under VA loading discussed in the previous sections are: (i) Significant interactions can occur. Cycles with a relatively high $S_{\max}$ can lead to a substantial reduction of the crack growth rate in subsequent cycles. (ii) Crack growth accelerations are possible, but crack growth retardations are generally overruling the acceleration. As a consequence, a non-interaction prediction may be expected to be a safe and conservative prediction. As mentioned in the introduction of this chapter, crack growth prediction as an engineering problem are relevant if fatigue cracks can affect the safety or economic use of a structure. A non-interaction crack growth prediction will then give a first indication about the possible duration of the crack growth period before a complete failure can be anticipated. It should be recalled that the result of such a prediction is depending on the crack growth rate data of the material, the stress-intensity factors used, and the load spectrum. The specimens used to obtain the basic crack growth data under CA loading should be representative for the conditions of the structure. It implies that the type of material should be the same, and preferably also the thickness of the material. The stress intensity factors, if not available in the literature, should be estimated or calculated. The load spectrum in service must also be available, either by analysis or measurements.

An important and practical question is whether a non-interaction prediction can be considered to be satisfactory. Two issues should be mentioned here. First, crack growth in service may be faster than predicted, due to a corrosive environment or an other time dependent phenomenon. This

problem was already addressed in Chapter 8 because it also applies to crack growth predictions under CA loading. Safety factors can be used to account for environmental effects, while exploratory tests on the environmental effect can be carried out for further guidance. The problem is considered again in Chapter 16. Second, another obvious problem is associated with the load spectrum. It is very well possible that a non-interaction prediction is highly conservative, the more so if infrequent high loads are part of the load spectrum. Engineers do not like to be conservative if it is not necessary. The following problem can arise: a non-interaction prediction gives a result with an unsatisfactory margin of safety, whereas a prediction accounting for crack closure gives a much longer crack growth life which could be sufficient. Whether this result is acceptable depends on the reliability of the prediction model. In such a case, it must be recommended to verify the prediction by selected service-simulation fatigue tests.

Aspects of the validity of prediction models

Prediction models for fatigue crack growth under VA loading have been discussed in Section 11.4. It was said that the empirical verification is often limited. Furthermore, the verification is sometimes presented as a comparison between predicted and empirical crack growth lives, a

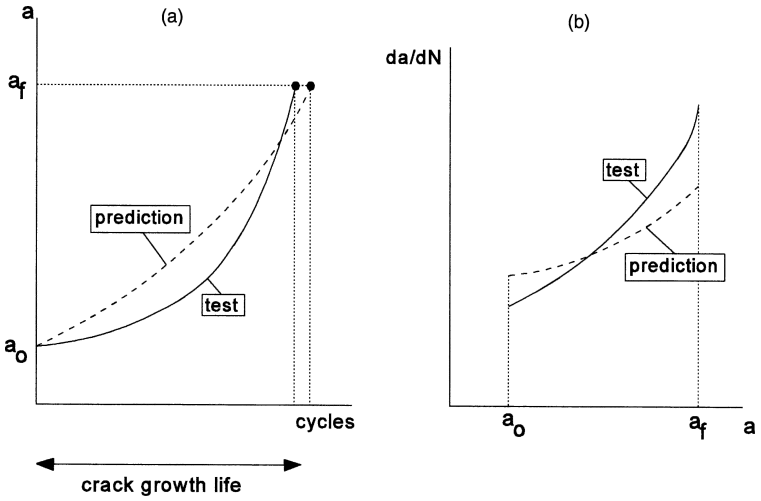

Fig. 11.21 Comparison between test result and prediction. Good agreement between crack growth lives, poor agreement between crack growth rates.

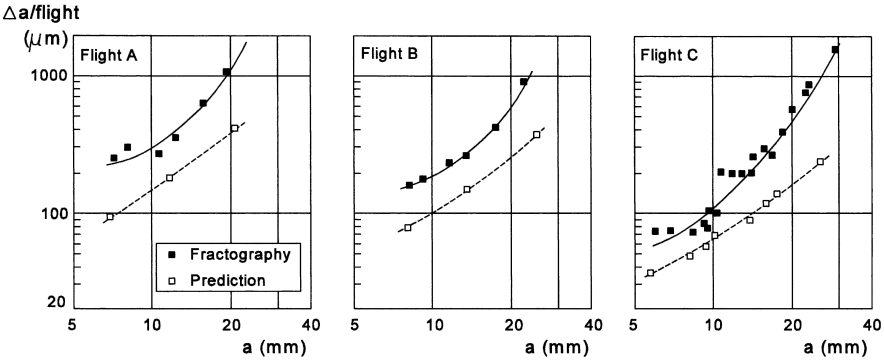

Fig. 11.22 Values of Δa in the most severe flights (A, B and C) of a flight-simulation fatigue test (miniTWIST) on an Al-alloy sheet specimen (2024-T3). Fractographic observations of the electron microscope (SEM) compared to predictions by the modified CORPUS model [45].

comparison used in Figure 11.19. However, as illustrated by Figure 11.21, a good agreement between crack growth lives (Figure 11.21a) can also be a result of an initially too high prediction of the crack growth rate $\mathrm{d}a/\mathrm{d}N$, which is compensated later by a too low prediction (Figure 11.21b). Verifications of prediction models should include a comparison of predicted and empirical crack growth rates. A still more detailed comparison can be made by fractographic striation measurements in the electron microscope. Such a comparison was made for fatigue crack grown under flight-simulation loading [45]. The crack extension in each of the more severe flights could be determined in the SEM by fractographic analysis, which required some skill and experience. As shown by the results in Figure 11.22, the crack extension in the more severe flights was considerably larger than predicted by the modified CORPUS model, although the agreement between the macroscopic crack growth rates, predicted and measured, was good. This is not inconsistent because the number of most severe flights in a flight-simulation test is small. An incorrect prediction for these severe flights has a small effect on the overall prediction. It implies that the crack growth prediction was satisfactory from an engineering point of view, but not from a physical point of view. A physical verification of a prediction model also requires a comparison on a microscopic level. Recall that such observations were essential to reveal the occurrence of delayed retardation in Figure 11.9.

Two arguments can be considered to explain the discrepancy for the severe flights in Figure 11.22; first, the larger Δa for primary plastic deformation discussed below, and second, an incompatible crack front orientation.

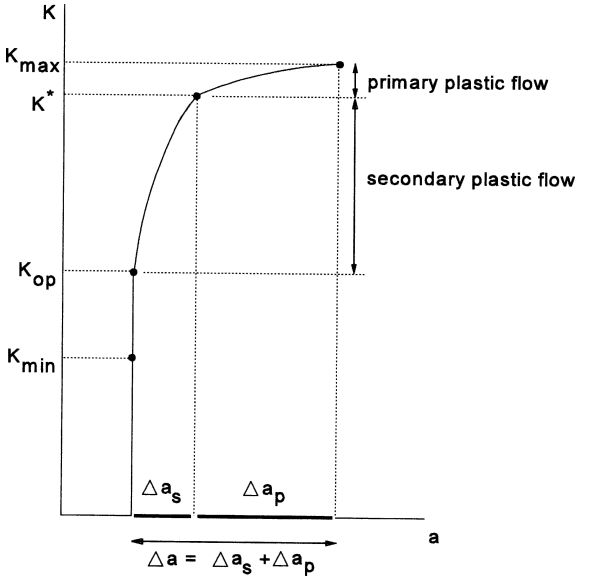

Fig. 11.23 Different crack increments during secondary and primary plastic deformation of crack tip plastic zone. Concept of De Koning [44].

As part of the CORPUS model, De Koning [26] introduced primary plastic deformation and secondary plastic deformation. Primary plastic deformation occurs at the crack tip if plastic deformation penetrates into elastic material which has not yet seen any plastic deformation by previous load cycles. Secondary plastic deformation refers to crack tip plasticity that remains inside a primary plastic zone. More recently De Koning and Dougherty [44] have proposed that crack extension during primary plastic deformation is much more effective than during secondary plastic deformation. In a load cycle, plastic deformation and crack extension will always start with secondary plastic deformation, see Figure 11.23.[15] If $S_{\max}$ is high enough, primary plastic deformation will occur after $K > K^*$. Crack extension, as long as $K < K^*$, will occur in agreement with a Paris type equation and a related crack growth mechanism. Above K^* crack extension will occur as a kind of stable crack growth under a quasi-statically increasing load. This could be a sound idea, which is supported by some empirical evidence, including fractographic observations [46, 47].

It may be expected that crack growth prediction models for VA loading will see further developments in the future. Also, more empirical verification

[15] In [44] a threshold level, slightly above K_{op}, is introduced. It is omitted here because it is not essential for the present discussion.

programs should validate wider applications to more load spectra and materials. This should also show which empirical constants are essential for tuning prediction models for specific applications. In view of the present qualitative understanding about interaction effects and the fatigue mechanism, the development of a generally valid and quantitative prediction model is still a problem for the future.

11.6 Major topics of the present chapter

The present chapter is dealing with fatigue crack growth of macrocracks under VA loading.

1. Significant interaction effects can occur during fatigue crack growth under VA loading. It implies that the crack growth rate ($\mathrm{d}a/\mathrm{d}N$) in a cycle is dependent on the load history of the preceding cycles, and it is not necessarily the same as in a CA test.
2. A load cycle with a high $S_{\max}$ (an overload, OL) can significantly reduce the crack growth rate in subsequent cycles (positive interaction effect). A load cycle with a low $S_{\min}$ (an underload, UL) can slightly increase the crack growth rate, while it can also reduce the retardation effect of previous OLs (negative interaction effects). In general, the positive interaction effects will overrule the negative ones during crack growth under service load spectra. As a result, non-interaction predictions for fatigue crack growth under VA loading will usually give conservative results.
3. Plasticity induced crack closure is a significant phenomenon to explain interaction effects. Experiments with simple VA-load histories have essentially contributed to understanding these effects. Similar interaction effects occur during more complex service simulating load histories.
4. Larger interaction effects occur in materials with a relatively low yield stress and in thinner materials, due to larger crack tip plastic zones.
5. Three types of prediction models for fatigue crack growth under VA loading have been proposed in the literature; yield zone models, crack closure models and strip yield models. The yield zone models do not agree with the present knowledge of interaction effects. The crack closure models account for the occurrence of plasticity induced crack closure and the transition of plane strain to plane stress. The strip yield models are the most sophisticated models, which include calculations

of plasticity induced crack closure. These models predict delayed retardation after an OL. The calculation algorithm of the strip yield models is complicated.

6. Empirical verification of prediction models is unfortunately rather limited. Verifications should not be restricted to predictions on crack growth lives, but should include predictions on crack growth rate as a function of crack length. Non-interaction predictions should also be made to indicate whether significant interaction effects occurred. Fractographic observations are recommended for investigations on prediction models.
7. Crack growth predictions for practical engineering problems should be validated by service-simulation fatigue tests.

References

1. Schijve, J., *Fatigue crack propagation in light alloy sheet material and structures*. Advances in Aeronautical Sciences, Vol. 3, Pergamon Press (1961), pp. 387–408.
2. Schijve, J., *Observations on the prediction of fatigue crack propagation under variable-amplitude loading*. Fatigue Crack Growth under Spectrum Loads, ASTM STP 595 (1976), pp. 3–23.
3. Mills, W.J. and Hertzberg, R.W., *The effect of sheet thickness on fatigue crack retardation in 2024-T3 aluminum alloy*. Engrg. Fracture Mech., Vol. 7 (1975), pp. 705–711.
4. Petrak, G.S., *Strength level effects on fatigue crack growth and retardation*. Engrg. Fracture Mech., Vol. 6 (1974), pp. 725-733.
5. Dahl, W. and Roth, G., *On the influence of overloads on fatigue crack propagation in structural steels*. Paper Technical University Aachen (1979).
6. Ling, M.R. and Schijve, J., *Fractographic analysis of crack growth and shear Lip development under simple variable-amplitude loading*. Fatigue Fract. Engng Mater. Struct., Vol. 13 (1990), pp. 443–456.
7. Schijve, J., *Four lectures on fatigue crack growth*. Engrg. Fracture Mech., Vol. 11 (1979), pp. 176–221.
8. Chermahini, R.G., Shivakumar, K.N. and Newman, Jr., J.C., *Three dimensional finite-element simulation of fatigue-crack growth and closure. Mechanics of Fatigue Crack Closure*. J.C. Newman, Jr. and W. Elber (Eds.), ASTM STP 982 (1988), pp. 398–413.
9. Grandt, A.F., *Three-dimensional measurements of fatigue crack closure*. NASA-CR-175366, Washington (1984).
10. Sunder, R. and Dash, P.K., *Measurement of fatigue crack closure through electron microscopy*. Int. J. Fatigue, Vol. 4 (1982), pp. 97–105.
11. McEvily, A.J., *Current Aspects of Fatigue*. Appendix: Overload Experiments. Fatigue 1977 Conference, University of Cambridge (1977).
12. Schijve, J., *Fatigue damage accumulation and incompatible crack front orientation*. Engrg. Fracture Mech., Vol. 6 (1974), pp. 245–252.

13. Stubbington, C.A. and Gunn, N.J.F., *Effects of fatigue crack front geometry and crystallography on the fracture toughness of an Ti-6Al-4V alloy*. Roy. Aero. Est., TR 77158, Farnborough (1977).
14. Ryan, N.E., *The influence of stress intensity history on fatigue-crack growth*. Aero. Research Lab., Melbourne. Report ARL/Met. 92 (1973).
15. Schijve, J., *Effect of load sequences on crack propagation under random and program loading*. Engrg. Fracture Mech., Vol. 5 (1973), pp. 269–280.
16. Saff, C.R. and Holloway, D.R., *Evaluation of crack growth gages for service life tracking*. Fracture Mech., R. Roberts (Ed.), ASTM STP 743 (1981), pp. 623-640.
17. Schijve, J., *Fundamental and practical aspects of crack growth under corrosion fatigue conditions*. Proc. Inst. Mech. Engrs., Vol. 191 (1977), pp. 107–114.
18. Unpublished results, National Aerospace Laboratory NLR, Amsterdam.
19. Wanhill, R.J.H., *The influence of starter notches on flight simulation fatigue crack growth*. Nat. Aerospace Lab. NLR, Amsterdam, Report MP 95127 (1995).
20. Broek, D., *Elementary Engineering Fracture Mechanics*, 4th edn. Martinus Nijhoff Publishers, the Hague (1985).
21. Schijve, J., Vlutters, A.M., Ichsan, S.P. and ProvoKluit, J.C., *Crack growth in aluminium alloy sheet material under flight-simulation loading*. Int. J. Fatigue, Vol. 7 (1985), pp. 127–136.
22. Schijve, J., *The significance of flight simulation fatigue tests*. Durability and Damage Tolerance in Aircraft Design, A. Salvetti and G. Cavallini (Eds.), EMAS, Warley (1985), pp. 71–170.
23. Willenborg, J. Engle, R.M. and Wood, H.A., *A crack growth retardation model using an effective stress concept*. AFFDL-TR71-1, Air Force Flight Dynamic Laboratory, Wright-Patterson Air Force Base (1971).
24. Wheeler, O.E., *Spectrum loading and crack growth*. J. Basic Engrg., Vol. 94 (1972), pp. 181–186.
25. Baudin, G. and Robert, M., *Crack growth life time prediction under aeronautical type loading*. Proc. 5th European Conf. on Fracture, Lisbon (1984), pp. 779–792.
26. de Koning, A.U., *A simple crack closure model for prediction of fatigue crack growth rates under variable-amplitude loading*. Fracture Mechanics, R. Roberts (Ed.), ASTM STP 743 (1981), pp. 63–85.
27. Padmadinata, U.H., *Investigation of crack-closure prediction models for fatigue in aluminum sheet under flight-simulation loading*. Doctor Thesis, Delft University of Technology, Delft (1990).
28. Aliaga, D. Davy, A. and Schaff, H., A *simple crack closure model for predicting fatigue crack growth under flight simulation loading*. Durability and Damage Tolerance in Aircraft Design, A. Salvetti and G. Cavallini (Eds.). EMAS, Warley (1985), pp. 605–630.
29. Padmadinata, U.H. and Schijve, J., *Prediction of fatigue crack growth under flight-simulation loading with the modified CORPUS model*. Advanced Structural Integrity Methods for Airframe Durability and Damage Tolerance, C.E. Harris (Ed.). NASA Conf. Publ. 3274 (1994), pp. 547–562.
30. Ichsan S. Putra, *Fatigue crack growth predictions of surface cracks under constant-amplitude and variable-amplitude loading*. Doctor thesis, Delft University of Technology (1994).
31. Newman Jr., J.C. and Armen, H., *Elastic-plastic analysis of a propagating crack under cyclic loading*. AIAA J., Vol. 13 (1975), pp. 1017–1023.
32. Ohji, K., Ogura, K. and Ohkubo, Y., *Cyclic analysis of a propagating crack and its correlation with fatigue crack growth*. Engrg. Fracture Mech., Vol. 7 (1975), pp. 457–463.

33. Dugdale, D.S., *Yielding of steel sheets containing slits*. J. Mech. Phys. Solids, Vol. 8 (1960), pp. 100–104.
34. Führing, H. and Seeger, T., *Structural memory of cracked components under irregular loading*. Fracture Mechanics, C.W. Smith (Ed.). ASTM STP 677 (1979), pp. 1144–1167.
35. Führing, H. and Seeger, T., *Dugdale crack closure analysis of fatigue cracks under constant amplitude loading*. Engrg. Fracture Mech., Vol. 11 (1979), pp. 99–122.
36. Dill, H.D. and Saff, C.R., *Spectrum crack growth prediction method based on crack surface displacement and contact analysis*. Fatigue Crack Growth under Spectrum Loads, ASTM STP 595 (1976) pp. 306–319.
37. Dill, H.D., Saff, C.R. and Potter, J.M., *Effects of fighter attack spectrum and crack growth*. Effects of Load Spectrum Variables on Fatigue Crack Initiation and Propagation, D.F. Bryan and J.M. Potter (Eds.). ASTM STP 714 (1980), pp. 205–217.
38. Newman, Jr., J.C., *A crack-closure model for predicting fatigue crack growth under aircraft spectrum loading*. Methods and Models for Predicting Fatigue Crack Growth under Random Loading, J.B. Chang and C.M. Hudson (Eds.). ASTM STP 748 (1981), pp. 53–84.
39. Dougherty, D.J., de Koning, A.U. and Hillberry, B.M., *Modelling high crack growth rates under variable amplitude loading*. Advances in Fatigue Lifetime Predictive Techniques, ASTM STP 1122 (1992), pp. 214–233.
40. Wang, G.S. and Blom, F. *A strip model for fatigue crack growth predictions under general load conditions*. Engrg. Fract. Mech., Vol. 40, (1991), pp. 507–533.
41. Bos, M.J., *Development of an improved model for the prediction of fatigue crack growth in helicopter airframe structure*. Proc. 24th ICAF Symposium, Naples, 16–18 May 2007, Vol. 1, L. Lazzeri and A. Salvetti (Eds.) (2007).
42. Skorupa, M. and Machniewicz, T., *Some results on the strip yield model performance*. Paper presented at the seminar held at TU Delft, 12 June 2007. To be published.
43. de Koning, A.U. and Liefting, G., *Analysis of crack opening behavior by application of a discretized strip yield model*. Mechanics of Fatigue Crack Closure, J.C. Newman, Jr. and W. Elber (Eds.). ASTM STP 982 (1988), pp. 437–458.
44. de Koning, A.U. and Dougherty, D.J., *Prediction of low and high crack growth rates under constant andvariable amplitude loading*. Fatigue Crack Growth under Variable Amplitude Loading, J. Petit et al. (Eds.). Elsevier (1989), pp. 208–217.
45. Siegl, J., Schijve, J. and Padmadinata, U.H., *Fractographic observations and predictions on fatigue crack growth in an aluminium alloy under miniTWIST flight-simulation loading*. Int. J. Fatigue, Vol. 13 (1991), pp. 139–147.
46. Schijve, J., *Fundamental aspects of predictions on fatigue crack growth under variable-amplitude loading*. Theoretical Concepts and Numerical Analysis of Fatigue, A.F. Blom and C.J. Beevers (Eds.). EMAS (1992), pp. 111–130.
47. Schijve, J., *Fatigue crack growth under variable-amplitude loading*. Fatigue and Fracture, American Society for Materials, Handbook Vol. 19, ASM (1996), pp. 110–133.

Some general references (see also [46, 47])

48. Skorupa, M., Machniewicz, T. and Skorupa, A., *Applicability of the ASTM compliance offset method to determine crack closure levels for structural steel*. Int. J. Fatigue, Vol. 29 (2007), pp. 1434–1451.
49. Skorupa, M. and Skorupa A., *Experimental results and predictions on fatigue crack growth in structural steel*. Int. J. Fatigue, Vol. 27 (2005), pp. 1016–1028.
50. Skorupa, M., *Load interaction effects during fatigue crack growth under variable-amplitude loading. A literature review. Part I: Empirical trends. Part II:*

Qualitative interpretations. Fatigue Fract. Engrg. Mater. Struct., Vol. 21 (1999) pp. 987–1006, Vol. 22 (1999), pp. 905–926.
51. Newman, Jr., J.C., Phillips, E.P. and Everett, Jr., R.A., *Fatigue analysis under constant- and variable-amplitude loading using small-crack theory*. NASA/TM-1999-209329 (1999).
52. Harter, J.A., *Comparison of contemporary fatigue crack growth (FGG) prediction tools*. Int. J. Fatigue, Vol. 21 (1999), pp. S181–S185.
53. Newman, Jr., J.C., Wu, X.R., Swain, M.H., Zhao, W., Phillips, E.P. and Ding, C.F., *Small-crack growth and fatigue life predictions for high-strength aluminium alloys. Part II: Crack closure and fatigue analyses*. Fatigue and Fracture of Engineering Materials and Structures, Vol. 23 (1999), pp. 59–72.
54. Wu, X.R., Newman, Jr., J.C., Zhao, W., Swain, M.H., Ding, C.F., and Phillips, E.P., *Small-crack growth and fatigue life predictions for high-strength aluminium alloys. Part I: Experimental and fracture mechanics analis*. Fatigue Fract. Engrg. Mater. Struct., Vol. 21 (1998), pp. 1289–1306.
55. Mitchell, M.R. and Landgraf. R.W. (Eds.), *Advances in Life Time Predictive Techniques*, ASTM STP 1122 (1992).
56. Newman, Jr., J.C. and Elber, W. (Eds.), *Mechanics of Fatigue Crack Closure*, ASTM STP 982 (1988).
57. *Fatigue Crack Growth under Spectrum Loads*, ASTM STP 595 (1976).